

Residual Neural Network applied to lightning classification in a modern lightning location network

Gabriel A.V.S Ferreira⁽¹⁾, Adonis F.R. Leal⁽¹⁾⁽²⁾, Elizabeth A. DiGangi⁽³⁾, Jeff Lapierre⁽³⁾, and Yanan Zhu⁽³⁾

(1) Graduate Program in Electrical Engineering, Federal University of Para, Belem 66075110, Brazil

(2) Langmuir Laboratory and Physics Department, New Mexico Institute of Mining and Technology, 801 Leroy Place, Socorro, NM 87801, USA

(3) AEM, Germantown, MD, USA

Abstract

In general, natural lightning flashes can be distinguished based on the charge that they neutralize (positive or negative), and if they reach the ground (Cloud-to-Ground – CG) or remain in the cloud (Intracloud – IC). On average, about 100 to 200 lightning strikes occur worldwide per second. This equates to roughly 8 million lightning strikes per day. Accurate lightning classification is crucial for identifying various types of thunderstorms and assessing their severity. Modern lightning location systems effectively capture a substantial portion of all lightning that occurs on Earth. However, due to the vast amount of data gathered, accurately classifying each lightning pulse poses a significant challenge. In this study, we evaluate the use of Earth Networks Total Lightning Network (ENTLN) data to develop a lightning classification model based on a Residual Neural Network (ResNet). We develop a new methodology to retrieve lightning electric field waveforms from ENTLN non-uniformly sampled data. The model was optimized to work in real-time, and its performance scores are accuracy = 95,2%, and F1-score = 92,6%.

1 Introduction

In general, there are two primary types of lightning: cloud-to-ground (CG), which reaches the ground, and intracloud (IC), which occurs within clouds and does not involve the ground. IC lightning comprises approximately three-quarters of all lightning discharges on Earth [1]. Lightning electromagnetic pulses generated by processes inside the cloud are different from those generated when lightning strikes the ground. Return-stroke electromagnetic pulses from ground strikes exhibit a short rise time and slow decay at distances beyond tens of kilometers [2], [3], [4], [5], whereas IC pulses have diverse waveforms, typically narrower than those from ground strikes.

Understanding lightning dynamics is challenging due to its stochastic nature, but accurate classification methodologies are crucial for analyzing thunderstorm behavior and predicting severe weather events. Studies have linked lightning characteristics to phenomena like aerosol concentration and severe weather manifestations [6], [7], [8], [9], [10], [11], [12], [13], [14], [15], [16], [17], emphasizing the relevance of precise lightning classification.

Traditional lightning classification methods using statistical analysis face limitations [18], [19], [20], prompting the exploration of Artificial Intelligence (AI) based approaches for this task, which have shown promising results in recent research. Machine learning algorithms like Support Vector Machines, Multi-Layer Perceptron, and Residual Neural Network (ResNet) have demonstrated superior performance in lightning classification compared to traditional methods [21], [22], [23], [24]. Continuous efforts

focus on enhancing classification accuracy through AI-based approaches, reflecting a shift towards incorporating AI into Lightning Location Systems for improved performance.

In December 2021, the Earth Networks Total Lightning Network (ENTLN) introduced its upgraded processor, featuring an enhanced classification algorithm based on logistic regression, a new propagation model, and improved regional data processing [25]. The processor's performance was assessed using natural and rocket-triggered lightning data from Florida, revealing improvements over the previous processor released in 2015. Accuracy in classifying natural lightning strokes increased from 91% to 94%, and in rocket-triggered lightning, from 86% to 88%. Location accuracy also improved, with median error reducing from 215 m to 92 m. The number of ENTLN pulses reported by the upgraded processor all over the world is about 50% higher than that of the previous one.

In this study, we evaluate the use of ENTLN data to train and test a ResNet model to perform lightning classification from electric field waveform data. The waveforms are reconstructed from the ENTLN sensors data and fed to the classification model. The ResNet is chosen based on previous attempts at lightning classification, as well as the used time window of 100 μ s [24].

2 Methodology and data

2.1 Data

The data used in this study is from the Earth Networks Total Lightning Network (ENTLN). ENTLN

consists of over 1800 sensors deployed in over 100 countries that detect wideband electric field signals emitted by intracloud (IC) and cloud-to-ground (CG) lightning [25].

The dataset consists of over 7600 pulses registered by ENTLN in the period from December 2018 to July 2021, which occurred in North America, South America, and Japan. Each pulse is labeled one of four classes: Positive Cloud-to-Ground (+CG), Positive Intracloud (+IC), Negative Cloud-to-Ground (-CG), and Negative Intracloud (-IC). Over 6800 of these pulses were classified manually by a person using a custom time delay comparison methodology, and the rest were +CG strokes verified and recorded by [26]. In this particular dataset, each pulse can contain from one up to hundreds of waveforms, depending on the number of stations that detected the same event. Due to this, the dataset is composed of over 374.000 waveforms detected by sensors located between 427 m to 2858 km away from the pulse location.

2.2 Preprocessing

We only used waveforms from stations within 500 km from the pulse location. Based on previous studies on lightning classification using electric field data [24], [27], we decided to use 100 μ s time windows. The reason is that ENTLN will classify the pulses in real-time, and according to [25], for real-time applications shorter time windows are preferable. The waveform peaks were set at around $t = 50$ μ s, leaving 50 μ s before and 50 μ s after the peak.

The waveforms captured by the ENTLN sensors undergo non-uniform sampling to efficiently manage data transfer and storage space. To retrieve the “original” electric field information we developed a new methodology in which we interpolate the non-uniformly sampled data, clean the artifacts, and include noise to the waveforms as shown in **Figure 1**.

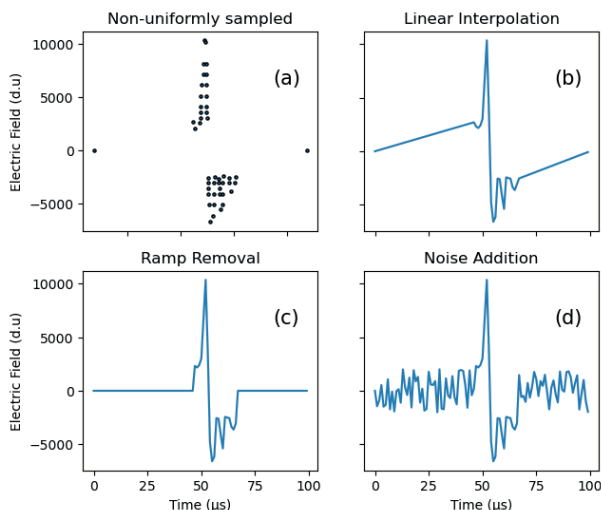


Figure 1 Preprocessing steps: (a) original non-uniformly sampled data, (b) linear interpolation, (c) removal of the ramp artifacts, and (d) noise addition.

We interpolate the data at 1MSPS rate, employing linear interpolation due to its simplicity. The resulting

waveform has 100 samples. Artifacts, characterized by ramps resulting from linear interpolation attempting to bridge distant data points, are removed by zeroing regions with gaps exceeding 50 μ s between original data points. Additionally, the entire waveform is scaled by the positive or negative peak value, constraining the maximum and minimum amplitudes between 1 and -1, respectively. Furthermore, random noise is intentionally introduced to enhance the robustness of the classification model, with the amplitude of this noise being related to the original noise level detected by the ENTLN sensors. Ultimately, the retrieved waveforms simplify the input stage of the classification model, improving its overall effectiveness. **Figure 2** shows waveform examples after preprocessing, for each lightning type.

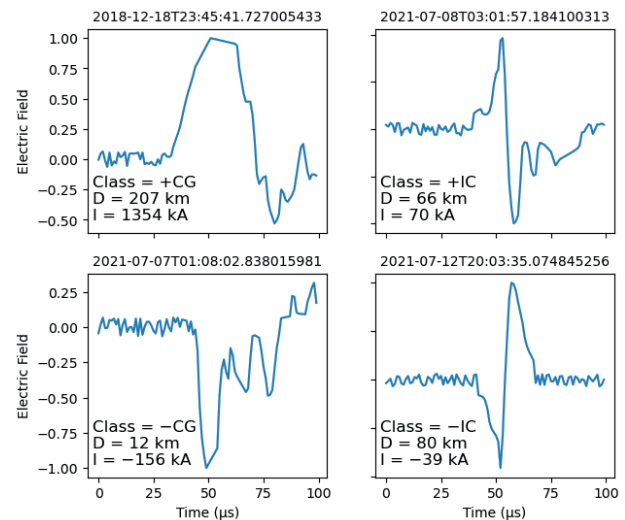


Figure 2 Waveform examples after preprocessing, for each lightning type.

Due to the nature of lightning occurrence, some classes are less represented than others. The +CG class, for example, represents less than 2.5% of the total number of waveforms. As the quality of the classification model is dependent on the quality of the dataset, distributions like this can result in less-than-optimal classifiers. To enhance the performance of the model, we use the Synthetic Minority Oversampling (SMOTE) Technique, introducing artificial instances between the original waveforms [28]. Furthermore, we use Random Undersampling (RUS) to remove random instances from the dataset and balance even more the data distribution. It's important to note that artificial instances were only added/removed to/from the training subset, leaving the test subset still imbalanced.

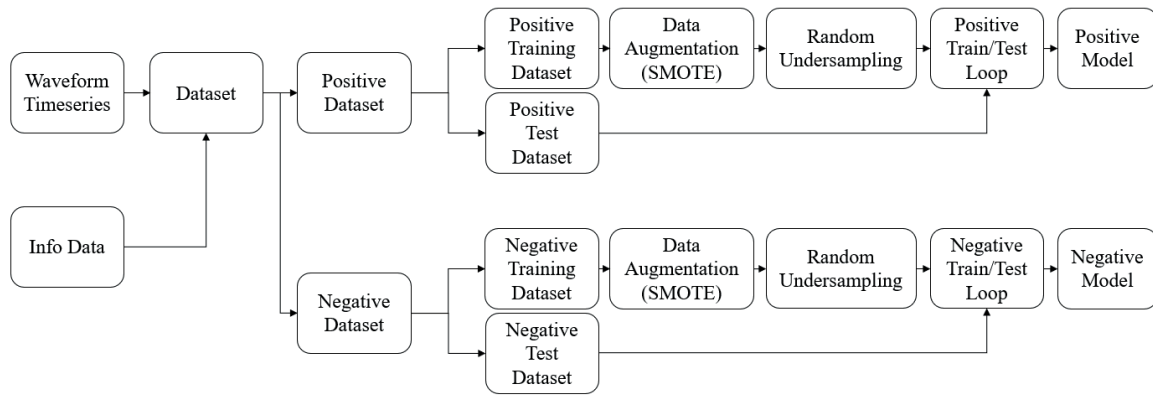


Figure 3 Block diagram of the training and testing processes.

2.3 Classification algorithm

The classification model employed in this study is the ResNet, short for Residual Neural Network. ResNets were devised to tackle the degradation problems encountered in deeper networks. This is achieved by incorporating shortcut connections, which consist of linear layers bridging the input and output of each residual block. These connections allow the model to learn more intricate data patterns, thereby enhancing its ability to accurately classify complex information [29].

Our ResNet follows the baseline presented in [24], [29], comprising 4 stacked residual blocks, each containing 3 convolutional blocks inside. Each residual block incorporates a linear layer connecting its input to its output. The convolutional blocks of the residual units work with kernel sizes of 8, 5, and 3, respectively, and corresponding filter sizes of 64, 128, and 128. A Batch Normalization layer follows the chained convolutions to speed up and stabilize the convergence of the model, and the ReLU activation function is added to increase the non-linearity response. Then, the features are fed up to a Global Average Pooling layer to reduce the number of weights needed in the final Dense layer that gives the probabilities of each label using the softmax activation function.

2.4 Training and testing

We opted to implement two distinct models tailored to each pulse polarity, effectively separating the classification process into negative and positive amplitude waveforms. This way, we can easily fine-tune the performance of each model, addressing the nuanced behaviors inherent to negative and positive datasets. The negative subset represents 43.1% of the total dataset, and the positive one represents 56.9%. SMOTE and RUS ratios were adjusted to cater to the unique requirements of each model, aiming to maximize their classification performance. The datasets are segregated both in the training and testing processes.

From the entire dataset, 80% of the pulses were drawn to compose the training subset and the remaining 20% were used for testing. Also, 20% of the training subset was used as the validation subset. The training epochs were

managed using the Early Stopping callback in Keras, which monitored the validation loss with a patience value of 50 epochs. The initial learning rate (LR) was set to 0.001 and was systematically reduced by the Reduce Learning Rate On Plateau callback in Keras. The LR reduction occurred when a validation loss plateau was identified, prompting the LR to halve after a patience value of 20 epochs. Additionally, the Model Checkpoint callback in Keras facilitated saving the latest best model by monitoring the validation loss. These callbacks effectively mitigate overfitting and streamline the training process.

The test loop consists of selecting the 5 nearest waveforms of the events and classifying them into four different classes. The ultimate classification label is given by the majority of the votes for all the waveforms. If an event has less than 5 waveforms, the loop works in the same way. The entire training and testing processes, including polarity segregation, and data augmentation are depicted by the block diagram in **Figure 3**.

3 Results and Discussion

The accuracy of the trained model was assessed only at the pulse level. For pulse level evaluation, accuracy was measured by comparing the model's predictions for individual pulses with the ground-truth pulse labels. The classification model was executed on a 64-bit Widows 10 laptop (processor: AMD Ryzen 5 5600H at 3.3 GHz) using Tensorflow and Keras on a Jupyter Python environment.

Our model demonstrates an improvement in classification accuracy compared to the one showcased in 2022 by [25], achieving an accuracy of 95.2% compared to 94%. The ResNet model achieved 95.2% accuracy, and F1 scores of 87.4%, 96.7%, 97.1%, and 89.0% in the classes +CG, -CG, +IC, and -IC, respectively. The macro averaged F1 score is 92.6%. Notably, recall values depicted in the confusion matrix for the ResNet classifier (**Figure 4**) are higher than 93%, for all classes. This indicates a consistent classification performance across all lightning types, underscoring the model's capacity to adapt to imbalanced datasets. When comparing our recall values to those derived from [30], it is evident that the ResNet classifier, employed

in conjunction with the new preprocessing methodology, yields improved results. This upgrade is especially visible in +CG (from 60.6% to 94.3%), -IC (from 76.8% to 93.2%) classes, and -CG (from 90.4% to 95.4%), where we have the least amount of data. +IC class suffers a reduction in performance from 97.0% to 95.5%.

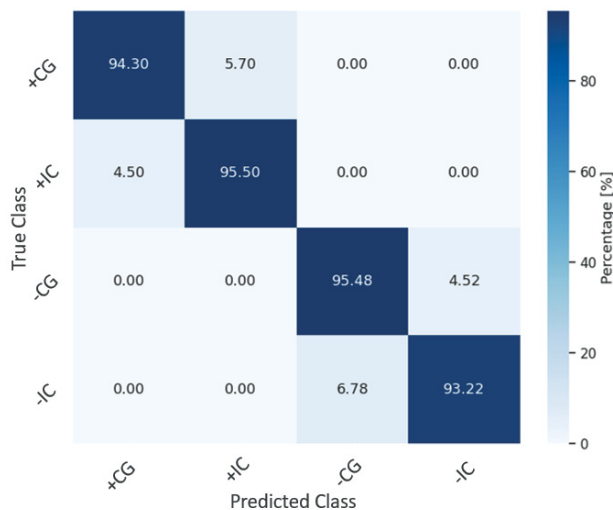


Figure 4 ResNet confusion matrix

Moreover, as depicted in **Figure 5**, it's notable that the negative model tends to overfit more rapidly than the positive model, as evidenced by the widening gap between validation and training loss scores. This can be traced back to the dataset distribution, where we have a better representation of positive lightning.

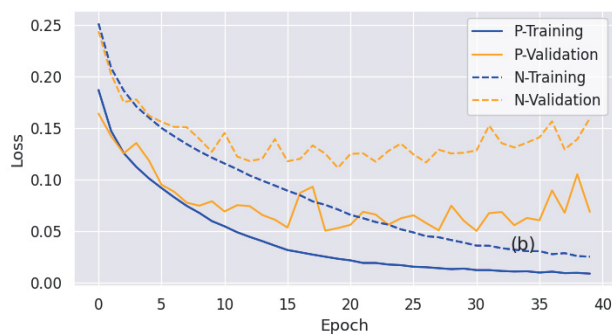


Figure 5 Training and Validation losses across the epochs

4 Summary

AI-based solutions to the lightning classification task represent a significant advancement over traditional methods. By using 100 μ s time window ENTNL waveforms, our classifier achieved an accuracy of 95.2% and a macro averaged F1 score of 92.6%, demonstrating consistently high performance across all types of lightning, with recall values exceeding 93% for each class. In our approach, a commonly misclassified type of lightning (+CGs) achieved an accuracy higher than 94%, which represents great improvements.

The new methodology employed to retrieve near-natural waveforms from ENTNL's non-uniformly sampled data proved invaluable in simplifying the input stage of the model, thus enhancing its overall effectiveness. By employing two distinct ResNet models, each dedicated to classifying a specific lightning polarity, we were able to finely adjust the SMOTE and RUS ratios, and deliver an overall well-balanced dataset, to cater to the requirements of each model, aiming to maximize their classification performance.

5 Acknowledgements

The authors would like to thank AEM for providing the truth dataset of pulses and their waveforms from the ENTNL, and Wu Ting of Gifu University for providing the EN R&D team with additional +CG data to augment the classification truth dataset.

6 Literature

- [1] V. A. Rakov, *Fundamentals of Lightning*. New York: Cambridge University Press, 2016.
- [2] Y. T. Lin et al., "Characterization of lightning return stroke electric and magnetic fields from simultaneous two-station measurements," *J Geophys Res Oceans*, vol. 84, no. C10, pp. 6307–6314, Oct. 1979, doi: 10.1029/JC084iC10p06307.
- [3] M. A. Haddad, V. A. Rakov, and S. A. Cummer, "New measurements of lightning electric fields in Florida: Waveform characteristics, interaction with the ionosphere, and peak current estimates," *Journal of Geophysical Research: Atmospheres*, vol. 117, no. D10, May 2012, doi: 10.1029/2011JD017196.
- [4] A. F. R. Leal and V. A. Rakov, "Characterization of Lightning Electric Field Waveforms Using a Large Database: 2. Analysis and Results," *IEEE Trans Electromagn Compat*, vol. 63, no. 6, pp. 1989–1997, Dec. 2021, doi: 10.1109/TEMC.2021.3062172.
- [5] A. Leal and V. Rakov, "Characterization of Lightning Electric Field Waveforms Using a Large Database: 1. Methodology," *IEEE Trans Electromagn Compat*, vol. 63, no. 4, pp. 1155–1162, Aug. 2021, doi: 10.1109/TEMC.2021.3059266.
- [6] J. N. Thomas, N. N. Solorzano, S. A. Cummer, and R. H. Holzworth, "Polarity and energetics of inner core lightning in three intense North Atlantic hurricanes," *J Geophys Res Space Phys*, vol. 115, no. A3, Mar. 2010, doi: 10.1029/2009JA014777.
- [7] T. J. Lang and S. A. Rutledge, "Cloud-to-ground lightning downwind of the 2002 Hayman forest fire in Colorado," *Geophys Res Lett*, vol. 33, no. 3, Feb. 2006, doi: 10.1029/2005GL024608.
- [8] N. D. Murray, R. E. Orville, and G. R. Huffines, "Effect of pollution from Central American fires on cloud-to-ground lightning in May 1998," *Geophys Res Lett*, vol. 27, no. 15, pp. 2249–2252, Aug. 2000, doi: 10.1029/2000GL011656.

- [9] W. A. Lyons, T. E. Nelson, E. R. Williams, J. A. Cramer, and T. R. Turner, "Enhanced Positive Cloud-to-Ground Lightning in Thunderstorms Ingesting Smoke from Fires," *Science* (1979), vol. 282, no. 5386, pp. 77–80, Oct. 1998, doi: 10.1126/science.282.5386.77.
- [10] K. P. Naccarato, O. Pinto, and I. R. C. A. Pinto, "Evidence of thermal and aerosol effects on the cloud-to-ground lightning density and polarity over large urban areas of Southeastern Brazil," *Geophys Res Lett*, vol. 30, no. 13, Jul. 2003, doi: 10.1029/2003GL017496.
- [11] S. M. Steiger, R. E. Orville, and G. Huffines, "Cloud-to-ground lightning characteristics over Houston, Texas: 1989–2000," *Journal of Geophysical Research: Atmospheres*, vol. 107, no. D11, Jun. 2002, doi: 10.1029/2001JD001142.
- [12] Y. Liu et al., "Aerosol Effects on Lightning Characteristics: A Comparison of Polluted and Clean Regimes," *Geophys Res Lett*, vol. 47, no. 9, May 2020, doi: 10.1029/2019GL086825.
- [13] A. O. Fierro, X.-M. Shao, T. Hamlin, J. M. Reisner, and J. Harlin, "Evolution of Eyewall Convective Events as Indicated by Intracloud and Cloud-to-Ground Lightning Activity during the Rapid Intensification of Hurricanes Rita and Katrina," *Mon Weather Rev*, vol. 139, no. 5, pp. 1492–1504, May 2011, doi: 10.1175/2010MWR3532.1.
- [14] A. R. Jacobson and M. J. Heavner, "Comparison of Narrow Bipolar Events with Ordinary Lightning as Proxies for Severe Convection," *Mon Weather Rev*, vol. 133, no. 5, pp. 1144–1154, May 2005, doi: 10.1175/MWR2915.1.
- [15] D. M. Suszcynsky and M. J. Heavner, "Narrow Bipolar Events as indicators of thunderstorm convective strength," *Geophys Res Lett*, vol. 30, no. 17, Sep. 2003, doi: 10.1029/2003GL017834.
- [16] S. Chkeir, A. Anesiadou, A. Mascitelli, and R. Biondi, "Nowcasting extreme rain and extreme wind speed with machine learning techniques applied to different input datasets," *Atmos Res*, vol. 282, p. 106548, Feb. 2023, doi: 10.1016/j.atmosres.2022.106548.
- [17] E. Williams et al., "The behavior of total lightning activity in severe Florida thunderstorms," *Atmos Res*, vol. 51, no. 3–4, pp. 245–265, Jul. 1999, doi: 10.1016/S0169-8095(99)00011-3.
- [18] A. F. R. Leal, V. A. Rakov, and B. R. P. Rocha, "Compact intracloud discharges: New classification of field waveforms and identification by lightning locating systems," *Electric Power Systems Research*, vol. 173, pp. 251–262, Aug. 2019, doi: 10.1016/j.epsr.2019.04.016.
- [19] A. Nag, M. J. Murphy, K. L. Cummins, A. E. Pifer, and J. A. Cramer, "Recent Evolution of the U.S. National Lightning Detection Network," *Tucson*, Mar. 2014.
- [20] C. J. Biagi, K. L. Cummins, K. E. Kehoe, and E. P. Krider, "National Lightning Detection Network (NLDN) performance in southern Arizona, Texas, and Oklahoma in 2003–2004," *Journal of Geophysical Research: Atmospheres*, vol. 112, no. D5, Mar. 2007, doi: 10.1029/2006JD007341.
- [21] Y. Zhu, P. Bitzer, V. Rakov, and Z. Ding, "A Machine-Learning Approach to Classify Cloud-to-Ground and Intracloud Lightning," *Geophys Res Lett*, vol. 48, no. 1, Jan. 2021, doi: 10.1029/2020GL091148.
- [22] J. Wang et al., "Classification of VLF/LF Lightning Signals Using Sensors and Deep Learning Methods," *Sensors*, vol. 20, no. 4, p. 1030, Feb. 2020, doi: 10.3390/s20041030.
- [23] D. R. Eads et al., "Genetic Algorithms and Support Vector Machines for Time Series Classification," B. Bosacchi, D. B. Fogel, and J. C. Bezdek, Eds., Dec. 2002, p. 74. doi: 10.1117/12.453526.
- [24] A. F. R. Leal, G. A. V. S. Ferreira, and W. L. N. Matos, "Performance Analysis of Artificial Intelligence Approaches for LEMP Classification," *Remote Sens (Basel)*, vol. 15, no. 24, p. 5635, Dec. 2023, doi: 10.3390/rs15245635.
- [25] Y. Zhu, M. Stock, J. Lapierre, and E. DiGangi, "Upgrades of the Earth Networks Total Lightning Network in 2021," *Remote Sens (Basel)*, vol. 14, no. 9, p. 2209, May 2022, doi: 10.3390/rs14092209.
- [26] T. Wu, D. Wang, and N. Takagi, "On the Intensity of First Return Strokes in Positive Cloud-To-Ground Lightning in Winter," *Journal of Geophysical Research: Atmospheres*, vol. 127, no. 22, Nov. 2022, doi: 10.1029/2022JD037282.
- [27] Y. Zhu, P. Bitzer, V. Rakov, and Z. Ding, "A Machine-Learning Approach to Classify Cloud-to-Ground and Intracloud Lightning," *Geophys Res Lett*, vol. 48, no. 1, Jan. 2021, doi: 10.1029/2020GL091148.
- [28] N. V. Chawla, K. W. Bowyer, L. O. Hall, and W. P. Kegelmeyer, "SMOTE: Synthetic Minority Over-sampling Technique," *Journal of Artificial Intelligence Research*, vol. 16, pp. 321–357, Jun. 2002, doi: 10.1613/jair.953.
- [29] Z. Wang, W. Yan, and T. Oates, "Time Series Classification from Scratch with Deep Learning Neural Networks: A Strong Baseline," in *2017 International Joint Conference on Neural Networks (IJCNN)*, Anchorage, May 2017, pp. 1578–1585.
- [30] E. DiGangi, Y. Zhu, J. Lapierre, and M. Stock, "Updates to the Earth Networks Total Lightning Network," in *Proceedings of the XXXVth URSI General Assembly and Scientific Symposium – GASS 2023*, Gent, Belgium: URSI – International Union of Radio Science, 2023. doi: 10.46620/UR-SIGASS.2023.1862.RNTA7845.



Gabriel A. V. S. Ferreira received the B.S. degree in electrical engineering from the Federal University of Para, Belem, Brazil, in 2023. He is currently working toward the M.S degree in electrical engineering at Federal University of Para.

His current research interests include lightning signal processing, lightning detection, investigation of Artificial Intelligence assisted solutions in lightning research.



Adonis F. R. Leal received the B.S., M.S and Ph.D. degrees in electrical engineering (Electronics and Power Systems) from the Federal University of Para (UFPA), Belem, Brazil in 2013, 2014 and 2018 respectively. From 2016 to 2017, he was a Visiting Research Scholar with the

Department of Electrical and Computer Engineering, University of Florida, Gainesville, FL, USA. From 2018 to 2022, he was an Assistant Professor in the Department of Electrical and Biomedical Engineering at the Federal University of Para, Belem, Brazil. He is currently an Assistant Professor in the Physics Department at New Mexico Tech, Socorro, NM, USA.

Elizabeth A. DiGangi

Jeff Lapierre

Yanan Zhu